Polymorphism in Pharmaceutical Solids

edited by
Harry G. Brittain
Discovery Laboratories, Inc.
Milford, New Jersey

MARCEL DEKKER, INC. NEW YORK · BASEL

ISBN: 0-8247-0237-9

This book is printed on acid-free paper.

Headquarters
Marcel Dekker, Inc.
270 Madison Avenue, New York, NY 10016
tel: 212-696-9000; fax: 212-685-4540

Eastern Hemisphere Distribution
Marcel Dekker AG
Hutgasse 4, Postfach 812, CH-4001 Basel, Switzerland
tel: 44-61-261-8482; fax: 44-61-261-8896

World Wide Web
http://www.dekker.com

The publisher offers discounts on this book when ordered in bulk quantities. For more information, write to Special Sales/Professional Marketing at the headquarters address above.

Current printing (last digit):
10 9 8 7 6 5 4 3 2 1

PRINTED IN THE UNITED STATES OF AMERICA

4

Structural Aspects of Hydrates and Solvates

Kenneth R. Morris

Purdue University
West Lafayette, Indiana

I. PHARMACEUTICAL IMPORTANCE OF CRYSTALLINE HYDRATES

The potential pharmaceutical impact of changes in hydration state of crystalline drug substances and excipients exists throughout the development process. The behavior of pharmaceutical hydrates has become the object of increasing attention over the last decade, primarily due (directly or indirectly) to the potential impact of hydrates on the development process and dosage form performance. Substances may hydrate/dehydrate in response to changes in environmental conditions, processing, or over time if in a metastable thermodynamic state [1].

It may not be practical or possible to maintain the same hydrate isolated at the discovery bench scale synthesis during scale-up activities for a hydrated compound. The choice of counterions to produce a more soluble salt form may also be dictated by the extent and type of hydration observed for a given salt and/or by the moisture level that may be safely accommodated by the dosage form [2].

The physicochemical stability of the compound may raise issues during preformulation. Some hydrated compounds may convert to an amorphous form upon dehydration and some may become chemically labile. This is true of cephradine dihydrate that dehydrates to become amorphous and undergoes subsequent oxidation. Other compounds may convert from a lower to a higher state of hydration yielding

forms with lower solubility. In any case, the resulting "new" forms would represent unique entities that, depending on the dosage form, might have to be maintained throughout the manufacturing process and in the clinic and would impact on the regulatory status of the compound. Most often this demands that the form (usually crystalline) be identified and characterized with respect to handling conditions during the early pre-IND stage of the development process.

As dosage form development proceeds, changes in hydration state can result in variable potencies depending on handling conditions during weighing steps, the kinetics of the hydration/dehydration process, and the environmental conditions during processing. Differences in powder flow can result from changes in crystal form and/or morphology that may accompany the hydration/dehydration process. This can affect content uniformity in solid processing either in the mixing process or during transfer to other processing equipment such as tablet presses. Aqueous granulation, particle size reduction, film coating, and tablet compression all provide opportunities to "trap" a compound in a metastable form that may "relax" to a more stable form at some unpredicted point in the life of a dosage form. Alternately, a kinetically favored but thermodynamically unstable form may be converted during these processes to a more stable and less soluble form.

During and after manufacturing, moisture from the environment or that sealed in the package may redistribute throughout the dosage form and change the hydration state(s). These changes can, in turn, visit the negative consequences discussed above for the bulk drug on the dosage form. These can be manifest as changes in tablet/capsule dissolution rates (and perhaps bioavailability), changes in lyophile reconstitution times, tablet capping, chemical instability, discoloration, and more. Of course, the potential for changes in hydration state also exists for many pharmaceutical excipients (such as lactose or magnesium stearate).

Such problems are typically magnified as both synthetic and dosage form production is scaled up. This may be caused by solvent limitations, heat transfer differences in production equipment, changes in raw materials and/or raw material suppliers, changes in processing times, and time and control constraints on product storage, to name a few.

The arguments just provided detail the potential issues around hydrates in the development process. The other consideration is the frequency with which hydrates are encountered in real life. Focusing on active drug substances, it is estimated that approximately one-third of the pharmaceutical actives are capable of forming crystalline hydrates [3]. A search of the Cambridge Structural Database (CSD) shows that approximately 11% of all the reported crystal structures contain molecular water [4]. This represents over 16,000 compounds. If organometallic compounds are excluded, this number drops to approximately 6,000 (3.8%), and the breakdown of these according to hydration number is shown in Fig. 1. This shows the expected trend in which monohydrates are most frequently encountered, and where the frequency decreases almost exponentially as the hydration number increases. The hemihydrate stoichiometry occurs approximately as frequently as the trihydrate, which should serve as a caution to explore fully the occurrence of fractional hydration. That is, an apparent stoichiometry of 0.6 water molecules could be a partially dehydrated monohydrate, or it

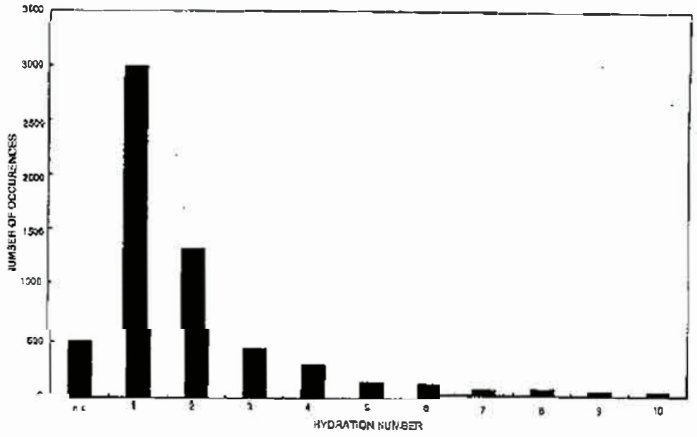

Fig. 1 Occurrence of various crystalline hydrate stoichiometries.

could be a hemihydrate with additional sorption due to defects or amorphous material.

The symmetry of these hydrate crystals follows fairly closely with that reported for organic structures overall [5]. Table 1 shows the breakdown for space groups, organized by crystal system, accounting for the top approximately 90% of the structures. $P2_1/c$ (number 14) is the most common space group here as with the general population of organic molecules contained in the CSD. It has been reported for inorganic species that hydrated structures are generally of lower symmetry than are their anhydrous counterparts [6]. This is attributed to the fact that the highest symmetry associated with the water molecule is C_{2v} and most inorganic structures are of higher symmetry. This is not obviously the case for organic structures. Regardless of the solvation state, organic molecules generally exhibit lower symmetry than do inorganic compounds, so the impact of the symmetry constraints imposed by water does not appear to be the controlling element. Further comparisons would be required to explore the phenomena fully.

Table 1 Space Groups for the Top 90% of Organic Crystalline Hydrates in the Cambridge Structural Database

Space group	Crystal system	Percent occurrence
P_{-1}	Triclinic	15.5
P_1	Triclinic	2.6
$P_{21/c}$	Monoclinic	23.2
P_{21}	Monoclinic	13.4
$C_{2/c1}$	Monoclinic	5.8
C_2	Monoclinic	2.8
P_{212121}	Orthorhombic	17.8
P_{bca}	Orthorhombic	2.3
P_{212121}	Orthorhombic	1.8
P_{na21}	Orthorhombic	1.8
P_{nma}	Orthorhombic	1.3
Unknown		1.2

II. HYDRATE THERMODYNAMICS

The equilibrium thermodynamics of stoichiometric hydrates has been described by several authors. The overview presented here is intended both to review the basic thermodynamics of crystalline hydrate formation/stability and to highlight the intrinsic differences between polymorphic systems and hydrate systems (a discussion of the kinetics of dehydration/hydration will be given in Section IV). The following description is a hybrid based on the work of Grant and Higuchi [7] and that of Carstensen [8].

A. Classical Higuchi/Grant Treatment

The equilibrium between a hydrate and an anhydrous crystal (or between levels of hydration) may be described by the following relationship.

$$A(\text{solid}) + mH_2O \leftrightharpoons A \cdot mH_2O(\text{solid}) \tag{1}$$

where

$$K_h = \frac{a[A \cdot mH_2O(\text{solid})]}{a[A(\text{solid})]a[H_2O]^m}$$

Here a represents the activity of the hydrate ($a[A \cdot mH_2O(\text{solid})]$) and anhydrate ($a[A(\text{solid})]$), respectively. When the water activity ($a[H_2O]$) is greater than the ratio

$$\frac{a[A \cdot mH_2O(\text{solid})]}{a[A(\text{solid})k_h]^{1/m}} \tag{2}$$

then the hydrate species is the stable form. The anhydrate species will be stable if the water activity is less than the ratio in Eq. (2). If the pure solids are taken as the standard states for the hydrate and anhydrous materials (i.e., as the states with unit activity), then $K_h = a[H_2O]^{-m}$ (and $m = 1$ for a monohydrate). So, clearly, the stability of a hydrate relative to the anhydrate (or lower hydrate) depends upon the activity of water in the vapor phase, or the partial vapor pressure or relative humidity (the ratio of the vapor pressure of water to the saturation vapor pressure at that temperature P/P_0). This straightforward thermodynamic description of hydrate equilibria is the key to un-

derstanding not only the stability of hydrated forms but the inherent differences between hydrates and polymorphs.

Just as the state of hydration depends upon the water vapor activity, so will the water activity (relative humidity, RH) in a closed system depend upon the state of hydration of the solid phase. These microenvironmental RH values can be of significance for the redistribution of moisture within a dosage form and/or package. An excellent illustration of this was given by Carstensen for sodium phosphate [9]. Figure 2 shows the relation between water vapor pressure (P) and the number of moles of water for the compound. Here it is seen that as water is added to a closed system, the compound takes it up until it no longer has any capacity in a given form (i.e., all of the solid is converted to a given hydrate). During this time, however, the RH of the system is constant. As more water is added, the RH rises until the critical value is reached that is sufficient to initiate the formation of the next higher hydration state. This cycle repeats as long as there are more states to be attained. Ultimately, the RH drifts up if the compound deliquesces. One would not, therefore, expect to maintain a constant RH with differences in water content in a system unless it contains hydratable components to buffer the changes. The type of behavior shown here is most common with inorganic compounds, but the principle is the same for

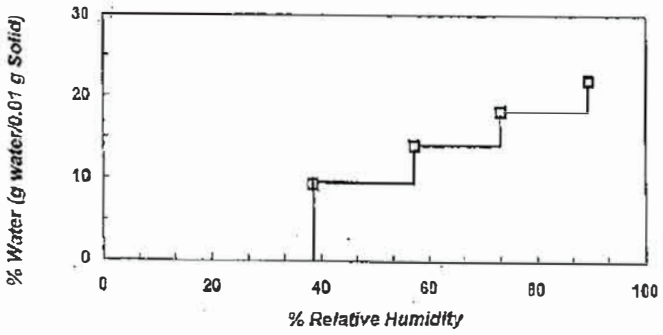

Fig. 2 Vapor pressure–hydration state diagram of sodium phosphate (reproduced with permission).

organic molecules even though the number of stable hydrates that form may be less.

B. Similarities and Differences Between Polymorphs and Hydrates

Hydrates and polymorphs are typically discussed together (as in this volume), and there are good reasons for this. In the scope of characterization of pharmaceuticals, many of the behaviors of polymorphic systems are at least apparently shared by compounds that can exist in various crystalline states of hydration. For the purposes of this chapter, such systems (including the anhydrous) will be referred to simply as hydrates. Members of both polymorphic and hydrate systems have different crystal structures and exhibit different x-ray powder diffraction patterns (XRPD), thermograms (DSC or TGA), infrared spectra, dissolution rates, hygroscopicity, etc. Interconversion between polymorphs or hydrates may occur as a function of temperature and/or pressure or be solution mediated. The potential for interconversion during processing, stability testing, and storage is, therefore, present for both polymorphs and hydrates. Given this long list of similar behaviors, it is generally proper that polymorphs and hydrates be addressed in the same general area of the pharmaceutical development process (for both technical and regulatory concerns).

The differences between polymorphs and hydrates are significant. The basis for all these differences is that polymorphs are different crystal structures of the same molecules(s) while hydrates are crystals of the drug molecule with different numbers of water molecules. As discussed above, the hydration state (and therefore the structure) of a crystalline hydrate is a function of the water vapor pressure (water activity) above the solid. Polymorphs, however, are typically only affected by changes in water vapor pressure if water sorption allows molecular motion, which in turn allows a reorganization into a different polymorph (i.e., a solution mediated transformation). This distinction is particularly important in defining the relative free energy of hydrates. A simple (only one molecule) anhydrous crystalline form is a one component system, and the free energy is, practically, specified by temperature and pressure. A crystalline hydrate is a two-component system and is specified

by temperature, pressure, and water activity. In both cases it is assumed that the activity of the pure solid is unity.

Consider the thermodynamic stability of a phase that crystallizes from water. If the phase is anhydrous (assuming no specific interaction between the molecule and the water), when the phase is removed from the solvent it is usually stable at that temperature (i.e., the free energy of the phase is independent of the solvent of origin). If the phase is hydrated, when it is removed from the solvent the situation changes completely. All that can be known is that the phase was thermodynamically stable at a water activity of approximately unity. Although it is a rule of thumb that the higher the hydration state that forms at a temperature the more thermodynamically stable, Grant et al. [10] have reported the opposite behavior. Once removed from the water, the activity of water needed to maintain the form (the critical activity) had to be determined by other methods. These may include water vapor sorption data or a titration of the amount of water in a cosolvent system [11]. A typical constant pressure G–T diagram (free energy vs. temperature, recalling that $\delta G/\delta T = -S$) for a polymorphic system is really analogous to a logarithm solubility vs. reciprocal temperature plot ($\ln X$ vs. $1/T$) for a system of hydrates (Figs. 3a and b). Alternatively, a G–T plot for a hydrate system at constant water activity is analogous. The relationship between free energy and the ideal solubility of a solid is seen from the following equation.

$$\Delta G = -RT \ln X \tag{3}$$

or

$$\ln X = \frac{\Delta S_f}{R} - \frac{\Delta H_f}{R} \cdot \frac{1}{T}$$

where ΔS_f and ΔH_f are the entropy and enthalpy of fusion at the melting point, respectively, and R is the gas constant. A plot of $\ln X$ against $1/T$ should yield a straight line with a negative slope equal to $-\Delta H_f/R$ and an intercept of $\Delta S_f/R$ for each phase. This conclusion assumes that the enthalpy of solution is equal to the enthalpy of melting at the melting point. A more general expression may be derived, but the reciprocal dependence of solubility and temperature is preserved. Just as with a

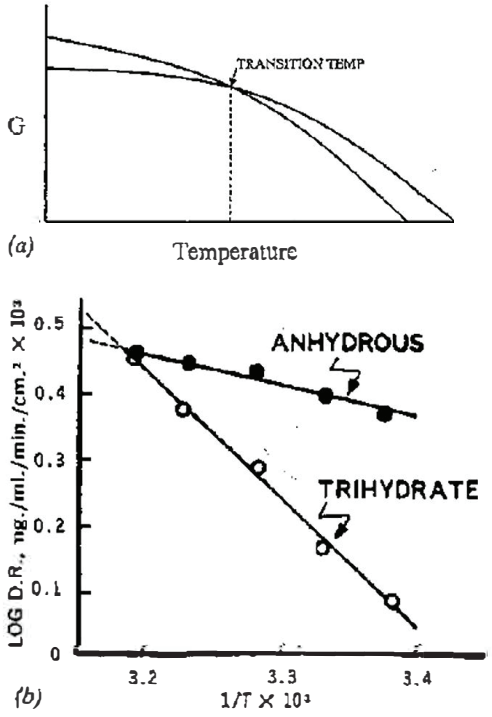

Fig. 3 (a) G–T diagram, two polymorphs, temperature plot. (b) Log dissolution vs. reciprocal temperature plot for ampicillin anhydrate and trihydrate (reproduced with permission).

G–T plot, the intersection of curves generated for two different crystalline phases represents a point of equal free energy and a transition temperature.

There are many implications of the relatively more complex structure of hydrates. As water is included or lost from the crystal structure, there must be a change in the volume of the unit cell (corrected for *Z*, the number of molecules per unit cell) at least as large as the volume

of the water molecule (15–40 Å^3) [12]. Although there is no study known to the author comparing the relative volume change between polymorphic pairs vs. hydrate pairs, it must be assumed that the trend would be that the volume change is larger for hydrates, which have to accommodate the additional volume occupied by the water molecules.

The obvious problem for pharmaceutical development is that the water activity can vary throughout the lifetime of the compound, and it is for this reason that knowledge of the water sorption behavior of active substances and excipients is so critical.

C. Hydrogen Bonding in Hydrates

The ability of water to form hydrogen bonds and hydrogen bonding networks gives it unique behavior with respect to colligative properties such as boiling and melting points. Similarly, hydrogen bonding between water molecules and drug molecules in the solid state dictates its role in the structure of all classes of crystalline hydrates (i.e., the ability of water to form cocrystals with the drug molecule). Water will, of course, be hydrogen bonded whenever physically possible. This may take the form of hydrogen bonding to other water molecules, with functional groups on other molecules, or to anions. Hydrogen bonding to other water molecules is common both in the crystal lattice and in interstitial cavities or channels. Hydrogen bonding to other moieties and anions in crystalline hydrates is primarily within the lattice. In addition, the lone pair electrons of the water oxygen may be associated with metallic cations present in many salts. This interaction is largely electrostatic in nature for the metal cations common to pharmaceutics (Na, Ca, K, Mg). These main-group metal ions lack the d-orbitals of suitable energy that are necessary to form coordinate covalent or coordination bonds that ions of the transition series form with oxygen. It is often stated that Mg(II) has a coordination number of 4, but this is a result of packing (or geometric) restrictions arising when fitting water molecules around the cation in response to the electrostatic attraction. Since these "bonds" are mostly electrostatic in nature, they are not properly described by a molecular orbital but are best defined by classical electrostatics [13]. These "bonds" are often stronger than hydrogen bonds but exist with less directional dependence. A typical water hydrogen

bond is on the order of 4.5 kcal/mol, whereas a sodium–oxygen lone pair electrostatic interaction can be four to five times stronger. These bonds also exert their influence through hydrogen bonds in the form of cooperative effects. The specific characteristics of the hydrogen bond are presented here in the formalism of Falk and Knop [6].

The ubiquitous hydrogen bonding of water is largely a result of its being both a hydrogen bond donor and acceptor. It may participate in as many as four hydrogen bonds, one from each hydrogen and one for each lone pair on the oxygen. Classification schemes based solely on the type of coordination of the water oxygen have been proposed [6]. As each bond is formed, it makes the other sites more attractive as partners for additional bonds. Hydrogen bond acceptors must be electronegative and include one of the following: oxygen atoms from other water molecules, oxygen and nitrogen atoms from other functional groups, and chlorine atoms. Hydrogen bond donors include protons on nitrogen, oxygen, and sulfur, of the types usually found on water, alcohols, amines, and the like.

Free water (vapor) has an OH bond length of 0.957 Å and an HOH angle of 104.52°. As soon as the molecule starts interacting with other molecules through hydrogen bonds, coordination, or other electrostatic "bonds", the molecule is distorted from its free conformation. The formation of hydrogen bonds weakens the OH bond, usually resulting in an increase in its length. This increase can be up to 0.01 Å for an exceptionally strong hydrogen bond, but it is more typically on the order of 0.01 to 0.02 Å for organic hydrates with hydrogen bond lengths of 2.7 to 2.9 Å (O—O distance).

The limits of length of a hydrogen bond are defined at the lower end by the van der Waals radii of the two atoms and at the upper end arbitrarily by the length of the weakest hydrogen bond observed. This can be seen more quantitatively by expressing the hydrogen bond distances shown in Fig. 4 in terms of the van der Waals radii.

$$R(\text{H—Y}) < r(\text{H}) + r(\text{Y}) - 0.20 \text{ Å} \tag{4}$$

and since $r(\text{H}) = 1.2$ Å,

$$R(\text{H—Y}) < r(\text{Y}) - 1.00 \text{ Å}$$

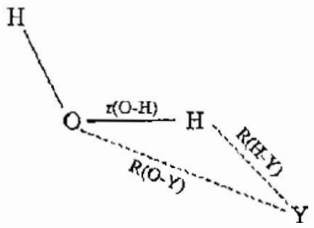

Fig. 4 Formalism used in the discussion of hydrogen bond strength and length. (From Ref. 6.)

The factor of 0.2 represents the combined experimental and statistical uncertainty. The compounds studied by Falk and Knop were inorganic and small organic hydrates [6]. Of the 129 compounds studied, only one failed this criterion. Often the hydrogen bond lengths are given as the O—Y (e.g., oxygen–oxygen or oxygen–chlorine) distances, because in x-ray diffraction studies it is often difficult or impossible to locate accurately the hydrogen atoms due to their inherently low scattering and their relatively high mobility. Because of the large cross sections, hydrogen atoms are often located by neutron diffraction studies. Under these circumstances, crystallographers will report the O—Y distance they know to be reliable, and geometric constraints may also be applied to such data.

$$R(\text{O—Y}) \leq R(\text{H—Y}) + r(\text{OH}) \tag{5}$$

substituting above, then setting $r(\text{OH}) = 0.98$ Å,

$$R(\text{O—Y}) \leq r(\text{Y}) + 1.98 \text{ Å}$$

As the electrostatic bond strength of the donor to the water oxygen (X) increases, the length of the H—Y bond decreases. This cooperative effect is also seen as the number of hydrogen bonds per water molecule increases. Hydrogen bonds prefer to be linear but may adopt a range of angles at the expense of the strength of the bond [6,15].

All of these aspects of water hydrogen bonding are evident in the infrared spectra of crystalline hydrates. When a molecule absorbs

infrared radiation, this energy is used to excite the molecule into higher vibrational energy level states. The occupancy of these higher states manifests itself in greater degrees of molecular vibration. The frequencies at which the molecule absorbs are a function of the mass of the bonded atoms, the geometry of the molecule, and the force constant (strength) of the bond. This relationship can be described by analogy to classical mechanics through Hooke's law, which states that the frequency of motion (ν) for a harmonic oscillator is inversely proportional to the square root of the reduced mass of the system (μ). The force constant (f, in units of dyn/cm) is the proportionality constant. Thus

$$\nu = \frac{1}{(2\pi c)}\left(\frac{f}{\mu}\right)^{1/2} \tag{6}$$

where c is the velocity of light in units of cm/s. As illustrated in Fig. 5, water in crystalline hydrates has nine potential degrees of freedom: two stretching modes (symmetric and asymmetric), one bending mode, three vibrational modes (hindered rotation), and three hindered transla-

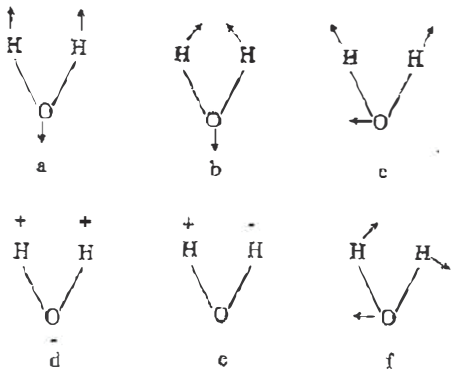

Fig. 5 Vibrational modes of water. Shown are the internal modes: (a) symmetric stretch, (b) bending, (c) asymmetric stretch, and the librational modes (d) wag, (e) twist, and (f) rock. Not shown are the three hindered translational modes.

tional modes. These vibrational modes and their characteristic absorption frequencies are presented in Table 2 and contrasted with those of water vapor.

The dominant feature in the infrared spectrum of a hydrate is band system associated with the O–H stretching frequencies between 4000 and 3000 cm^{-1}. These peaks are unusually intense due to the effect of hydrogen bonding on the changes in dipole moment that are associated with the wave functions describing the molecular motion. If an O–H stretching band is not observed, then no water is associated with the compound. When present, the contributing OH groups must be properly assigned to distinguish water from alcoholic, phenolic, hydroxide, or other interfering absorptions. This is accomplished by first assigning energy values to the known structure of the molecule from tables. If resolved, the presence of an H_2O bending frequency around 1600 cm^{-1} is proof that the sample contains water. Comparing this to the IR spectrum of the anhydrous material or the dehydrated sample shows which peaks in the region are due only to water. The IR spectra of ampicillin before and after dehydration exhibits such behavior.

Table 2 also shows that the OH stretching frequency of water occurs at lower wave numbers (longer wavelength and lower energy) in the crystal than in the vapor. This is due to the reduction of the force constant (f) by interaction of the water with neighboring groups, in particular hydrogen bonding and lone pair interactions involving the water oxygen. The weakening of the bond results in a slight elongation of the bond length, in the range of 0.01 to 0.02 Å [15]. This shift in

Table 2 Vibrational Modes of Water in Various Phases

Vibrational mode	Frequency in vapor phase (cm^{-1})	Frequency in solid phase (cm^{-1})
Stretching	3755.8 (symmetric) 3656.7 (asymmetric)	2850–3625
Bending	1594.6	1498–1732
Rotation/libration		355–1080
Translation		200–490

the OH stretching frequency of water can be used to evaluate the interaction energy between water and the other molecules. Specifically, the higher is the degree of water hydrogen bonding, the lower the frequency will be of the OH stretch. In fact, good correlation between OH stretching frequency and the length of hydrogen bonds is available for inorganics and very small organic crystals [14]. While repulsive lattice energy tends to increase this frequency, it typically yields only a very small shift. In large molecular crystals, however, the energetics become more complicated and the correlation is not as good. Adventitious adsorbed water tends to have broad peaks in the lower part of the frequency range. The broadening is due to the vibrational coupling between water molecules, and the lower frequencies are due to the multiple hydrogen bonds. This "dispersion of stretching frequencies" is analogous to the broadening of DSC peaks due to the multiple energetic environment that adventitious water can experience. If the water occupies only one type of crystal site, the DSC and IR peaks should be sharp relative to those of adventitious water. This is seen in the ampicillin example of the classification section. The O–H stretching peaks from water in the crystal lattice will occur at various frequencies depending upon the strength of the hydrogen bonding.

In addition to shifts in frequency and peak shape, peaks may become split owing to the interaction of the two water hydrogens if they participate in different hydrogen bonds. Therefore in some crystalline hydrates there may be two or more peaks associated with the OH stretching mode.

Metal cations affect the infrared absorption behavior in several ways. First, if the water oxygen is bound at the inner hydration sphere of the cation, polarization of the electron density causes stronger hydrogen bonds to be formed. This effect will lower the OH stretching frequency in a manner proportionate to the degree of bond strengthening, a decrease that can be up to 640 cm^{-1} in inorganic compounds [6,15]. Second, cation–water interaction can increase the bending frequencies (which are observed in the 1600 cm^{-1} region) by as much as 50 cm^{-1}. Finally, the bonds formed between the cation and the atoms in its inner coordination sphere will be observed as low-frequency modes below 400 cm^{-1}.

III. CLASSIFICATION OF HYDRATES

The combination of the vibrational mode information, the hydrogen bonding characteristics, and the thermodynamic relationships serves to form a clear picture as to why water can and does participate in hydrate formation with drug molecules. The possible structures that may result from such interactions are quite diverse. For practical purposes, an identification of types or classes of possible resulting structures is useful. Water is small enough to fill many commonly occurring periodic "voids" formed when larger molecules are packed, and it interacts through hydrogen bonds to overcome some of the entropy of mixing. The ability of the water molecules to self-associate, combined with the small size, allows them to fill larger periodic spaces conforming to different shapes. The characteristics give water a chameleon-like quality (also seen in protein hydration), which gives rise to "motifs" of water arrangements in crystal structures.

Crystalline hydrates have been classified by either structure or energetics [6]. The idea of the structural classification scheme presented here is to divide the hydrates into three classes that are discernible by the commonly available analytical techniques. The classification of crystalline hydrates of pharmaceutical interest by their structural characteristics is the most common, intuitive, and useful approach. A good classification system should direct the preformulation/formulation scientist to the characteristics of the particular class that will help in identifying a new sample, in selecting the proper form of the substance, and in estimating boundary conditions for safe handling (Table 3).

Table 3 Classification of Crystalline Hydrates

Class	Description
1	Isolated lattice sites
2	Lattice channels
−a	Expanded channels (non-stoichiometric)
−b	Lattice planes
−c	Dehydrated hydrates
3	Metal-ion coordinated water

An example of each class and the analytical manifestations of its crystalline structure will be presented in the succeeding sections. For this section, each class will be examined with respect to a specific example for which single crystal structure, DSC/TGA, XRPD, and IR data are available. Starting with the packing diagrams from the solved structure, the data from the other methods will be compared to that expected based on the information presented in the discussions above.

A. Class 1: Isolated Site Hydrates

These hydrate species represent the structures with water molecules isolated from direct contact with other water molecules by intervening drug molecules. To illustrate some of the characteristics of this hydrate class, consider the example of cephradine dihydrate [17], whose structure is shown in Fig. 6. This compound has the chemical formula $C_{16}H_{18}N_3O_4S$ (molecular weight 385.45) and is identified by the Cambridge reference code SQ22022. It crystallizes in the $P2_1$ space group and has the unit cell dimensions of a = 10.72 Å, b = 7.31 Å, and c = 11.87 Å. Finally, the cell volume is 908 Å^3, and its density is 1.41 g/cm^3.

The characterization of the crystal structure of cephradine dihydrate was particularly important because it becomes amorphous and very unstable upon dehydration [17]. Figure 7 shows the packing diagram of cephradine dihydrate, while Fig. 8 shows the measured and calculated XRPD patterns. Each unit cell contains two molecules of

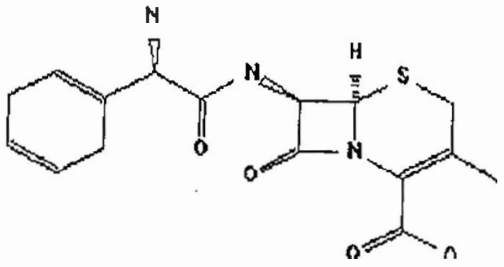

Fig. 6 Structure of cephradine.

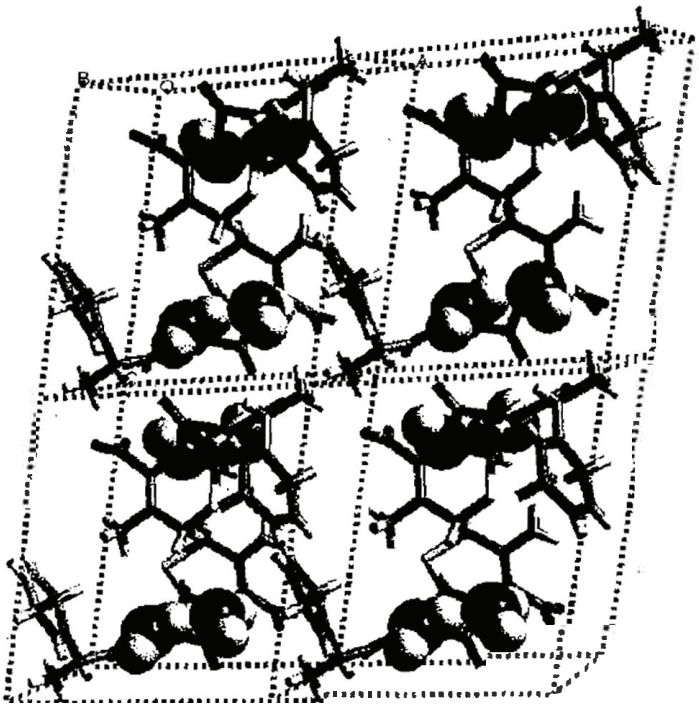

Fig. 7 Packing diagram from single crystal data for cephradine dihydrate. The van der Waals radii are included for the water hydrogens and oxygen. The pairs of water molecules reside in isolated lattice sites.

cephradine and four molecules of water. The diagram shows isolated pairs of water molecules arranged at intervals in the lattice. The two water molecules hydrogen bond with each other, and with the carbonyl, carboxyl, and amide groups on the two cephradine molecules.

No axis can be drawn between separate water pairs without passing through an intervening portion of the cephradine molecule. This means that a pair of water molecules on the surface may be easily

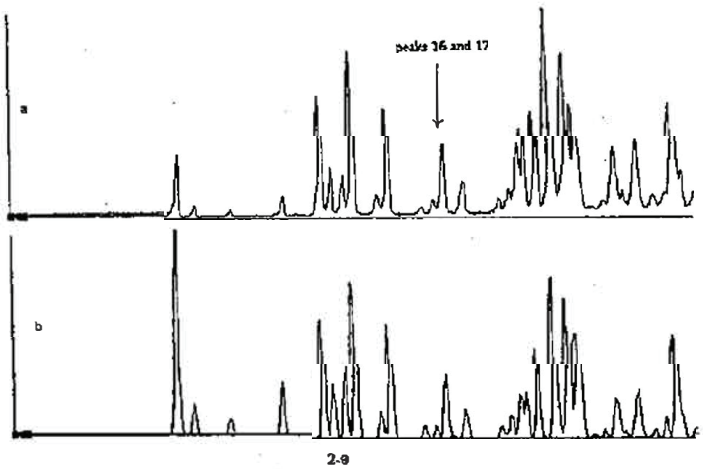

Fig. 8 (a) Measured and (b) calculated x-ray powder diffraction patterns for cephradine dihydrate.

lost, but the creation of the hole does not leave other water molecules accessible. Similarly, no network of hydrogen bonds exists solely involving water molecules on any axis through the crystal. The diagram has been constructed to show the water molecules with their van der Waals dimensions while the drug is in a stick representation. Areas that may appear void between pairs are actually filled by the electron clouds of the neighboring atoms. Since each pair is located in the same environment, it is expected that the interaction energy between each water molecule and its neighbor be similar (low energy dispersion).

This structure should yield sharp DSC endotherms, a narrow TGA weight loss range, and sharp O–H stretching frequencies in the infrared spectrum (Figs. 9a and b and 10). The DSC thermogram shows two incompletely resolved, but sharp, endotherms at approximately 100°C, and the TGA thermogram shows the anticipated sharp weight loss over a similar range. In addition, the onset of dehydration observed in the DSC curve is quite sharp. The diffuse reflectance infrared (DRIFT)

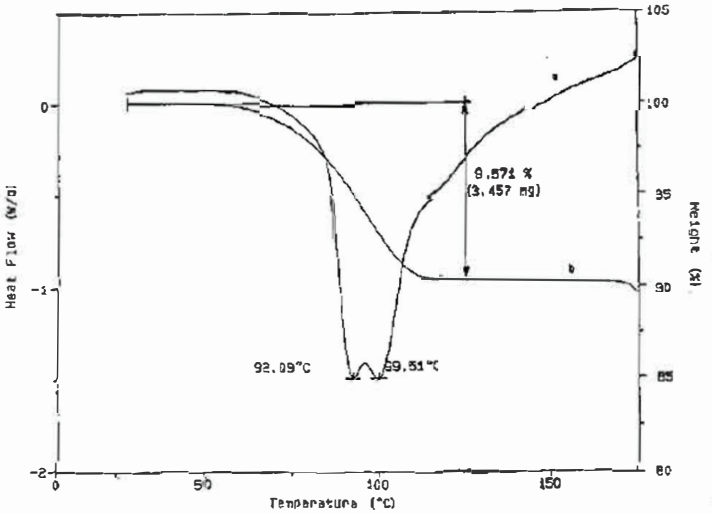

Fig. 9 (a) Differential scanning calorimetry and (b) thermogravimetric analysis thermograms for cephradine dihydrate.

spectrum of cephradine dihydrate shows sharp O–H stretches at approximately 3520 and 3425 cm^{-1} that are absent in the anhydrous material [17]. The thermal and spectroscopic data are seen to be consistent with the known single-crystal structure. Were the single crystal structure not available, the general features of the water association could have been deduced using the rationale previously developed.

B. Class 2: Channel Hydrates

Hydrates in this class contain water in lattice channels, where the water molecules included lie next to other water molecules of adjoining unit cells along an axis of the lattice, forming "channels" through the crystal. The empty channels are actually a conceptual construct, since a corresponding low-density structure with empty channels would not be

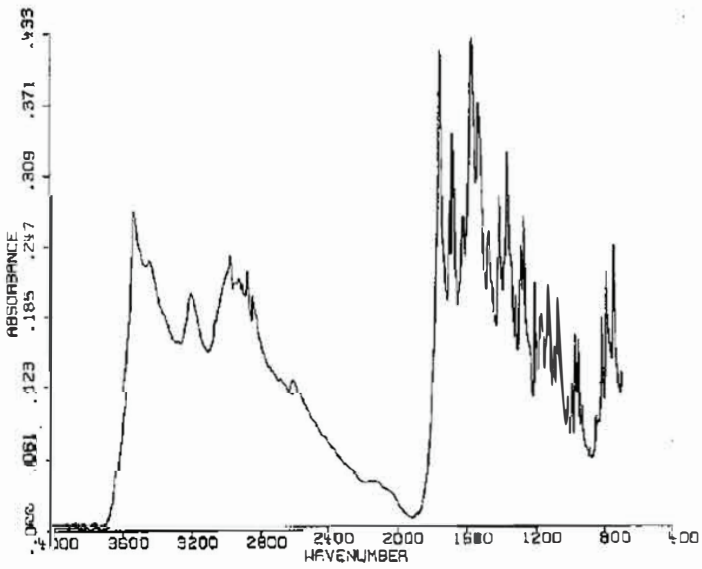

Fig. 10 Diffuse reflection infrared absorption (DRIFT) spectrum of cephradine dihydrate.

expected to be physically stable without some associated change in lattice parameters.

To illustrate some of the characteristics of the second hydrate class, we will examine the instance of ampicillin trihydrate [18,19], whose structure is shown in Fig. 11. This compound has the chemical formula $C_{16}H_{19}N_3O_4S$ (molecular weight 349.41) and is identified by the Cambridge reference code AMPCIH. It crystallizes in the $P2_12_12_1$ space group and has the unit cell dimensions of a = 15.49 Å, b = 18.89 Å, and c = 6.66 Å. Finally, the cell volume is 1949.4 Å^3, and its density is 1.37 g/cm^3.

Figure 12 shows the packing diagram, which consists of eight unit cells, and Figs. 13a and b show the measured and calculated XRPD patterns. As is obvious from the diagram, the water molecules line up

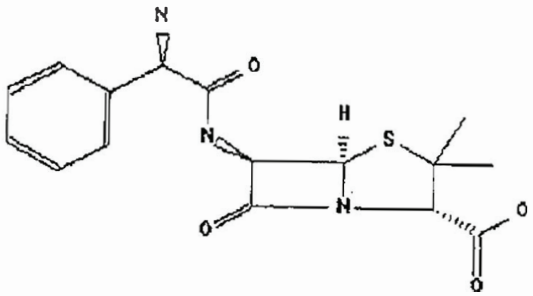

Fig. 11 Structure of ampicillin.

along the c screw axis. A channel of 3.5 Å would be formed if the water molecules were to leave without changing the structure. The water molecules occupy specific sites in the lattice (ordered water), as has been noted for cephradine. The water molecules are hydrogen bonded to four (or more) other water molecules and at least two ampicillin molecules through the carboxylate ion, the carbonyl on the β-lactam, the amino group, or through the ammonium group. Ampicillin trihydrate crystallizes as the zwitterion [19].

Examination of the DRIFT spectrum of ampicillin (Fig. 14) shows a sharp O–H stretching frequency at 3334 cm^{-1}, and an O–H bend at 1650 cm^{-1}, which are absent in the spectrum of the anhydrous form. The sharp O–H stretch indicates that the interaction energies between the OH groups on the water and the drug fall into the expected relatively narrow range. In addition, the band frequency is lower than that for cephradine, which suggests that the hydrogen bonding may be stronger in ampicillin. This is supported by the comparison of the DSC curves, which show dehydration at about 100°C for cephradine and 120°C for ampicillin.

The DSC/TGA data (Figs. 15a and b) also show one of the interesting characteristics of channel hydrate dehydration. Notice the early onset of dehydration for ampicillin compared to cephradine (isolated sites). Ampicillin loses water continuously to 125°C, while cephradine endotherms are very narrow even though the dehydration temperature of ampicillin is higher. This is due to dehydration beginning at the

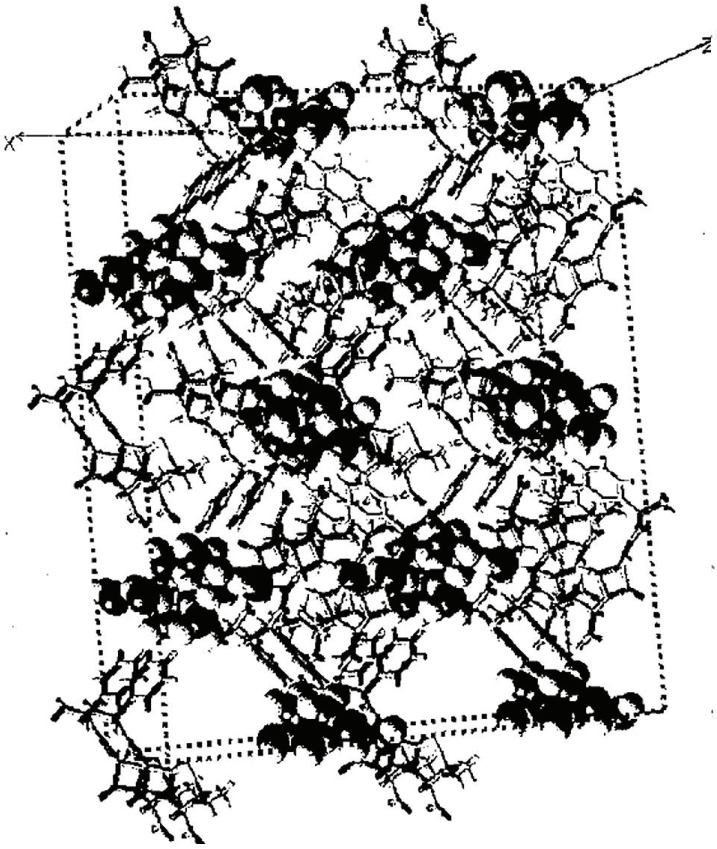

Fig. 12 Packing diagram for ampicillin trihydrate deduced from the single-crystal structural data. The van der Waals radii are included for the water hydrogens and oxygen, and the "channels" are along the screw axes.

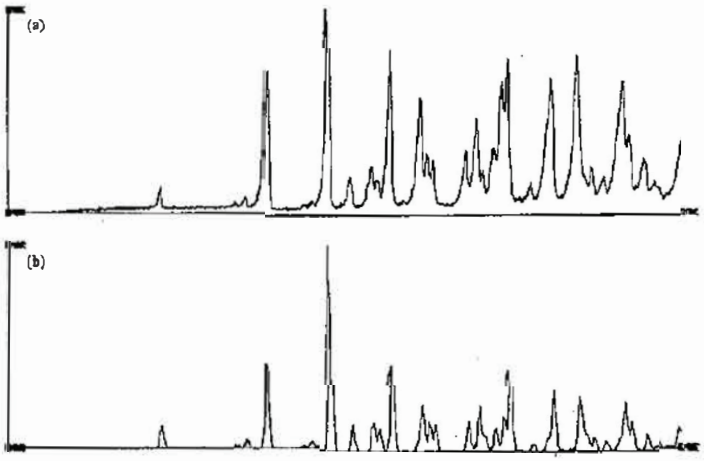

Fig. 13 (a) Measured and (b) calculated x-ray powder diffraction patterns for ampicillin trihydrate.

"ends" of the crystal and continuing toward the center along the channels. As the temperature increases so does the probability of losing the first water molecules on the surface at the channel ends. The loss of these water molecules leaves a channel for the next and sets up a thermodynamic gradient in the same direction. The drug molecules need not reorganize to lose many water molecules from the crystal. Using light microscopy, Byrn has observed and documented this phenomenon for ampicillin and theophylline [20]. As the crystal is heated on the microscope hot stage, the dehydration appears as a progressive darkening (increasing opacity) from the ends of the crystal toward the center along the c crystallographic axis. At some point in the dehydration, the crystal may either change its structure or become amorphous. Ampicillin would be recognizable as a channel hydrate based solely on microscopic/hot stage observations.

1. Expanded Channels

Another characteristic of some channel hydrates is that they may take up additional moisture in the channels when exposed to high humidity.

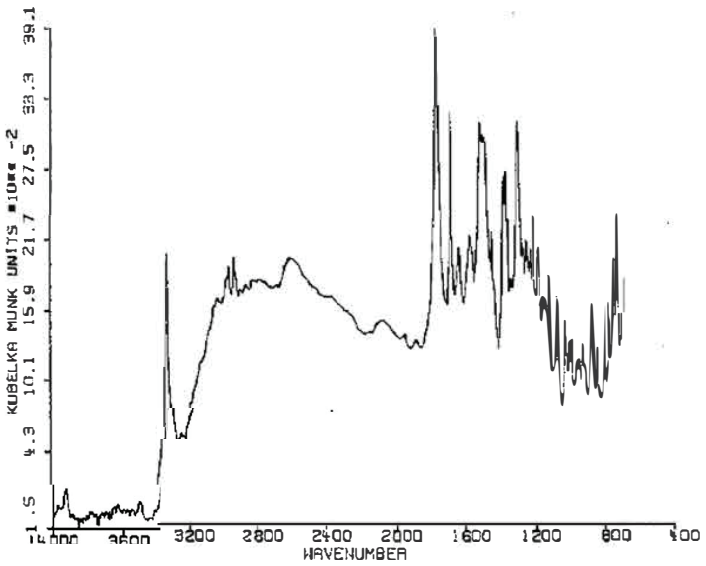

Fig. 14 Diffuse reflection infrared absorption (DRIFT) spectrum of ampicillin trihydrate.

As the hydration or dehydration proceeds, the crystal lattice may expand or contract by as much as 0.8 Å [21]. This lattice expansion must effect changes in the dimensions of the unit cell. This is manifested in the XRPD pattern as slight shifts in some or all of the scattering peaks. If the dimension increases, the associated peak is shifted to smaller 2-θ values, which correspond to larger d-spacings, and visa versa. This was shown qualitatively for chromylin sodium by Cox et al. [21]. As the chromylin absorbed more moisture, the lattice expanded to accommodate the additional water. The d-spacings and unit cell dimensions increased with water content, as determined by analysis of the film, but the structure was not solved for each level of hydration. Their subsequent model was used to determine the number of water molecules necessary to account for the observed expansion. As hydration contin-

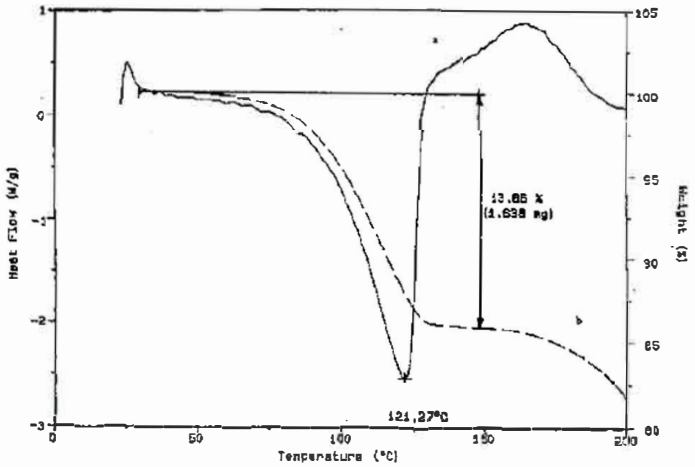

Fig. 15 (a) Differential scanning calorimetry and (b) thermogravimetric analysis thermograms for ampicillin trihydrate.

ues, the crystal expands until the changes are too large to maintain the same crystal structure. At this point, another crystal structure can result (with its own XRPD pattern), or it may revert to an amorphous material. This behavior is often observed with channel hydrates and warrants further division into subclasses having the characteristics of being non-stoichiometric or of continuously variable hydration.

Another example for which the single crystal structure was not known was (S)-4-[[[1-(4-fluorophenyl)-3-(1-methylethyl)-1H-indol-2-yl]-ethynyl]-hydroxyphosphinyl]-3]-hydroxy-butanoic acid, disodium salt (also known as SQ33600, whose structure is shown in Fig. 16); physical investigations provided considerable insight into the structure [22]. SQ33600 was found to take up moisture variably, lose it on exposure to low humidity (and/or heating), and appeared to undergo lattice expansion. Figure 17 shows the XRPD patterns for material stored at different relative humidities. It is clear that the largest changes take place in the low angle diffractions (larger d-spacings) as the degree of exposure to relative humidity increases. The same is true for several

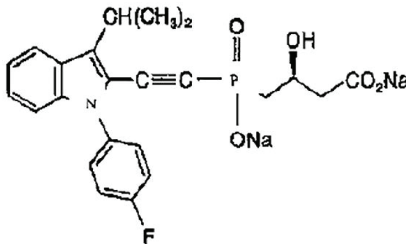

Fig. 16 Structure of (S)-4-[[[1-(4-fluorophenyl)-3-(1-methylethyl)-1H-indol-2-yl]-ethynyl]-hydroxyphosphinyl]-3]-hydroxybutanoic acid, disodium salt, SQ33600.

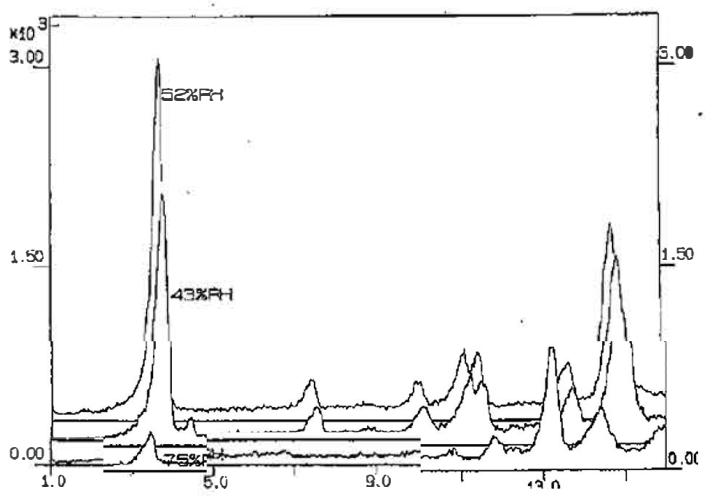

Fig. 17 X-ray powder diffraction patterns for SQ33600 at various relative humidity values.

other diffractions in material stored at 43% and 52% RH, while at 75% RH the structure has changed into something quite different (retaining only the low angle diffraction peaks in common). In fact, the material will deliquesce at a relative humidity of 75%.

2. *Planar Hydrates*

This subclass of crystalline hydrates has its water localized in a two-dimensional order, or plane. Figure 18 shows the packing diagram for sodium ibuprofen, where the waters of hydration are associated with the sodium ions localized in the a–c plane of the lattice. A similar structure has been reported for nedocromil zinc [23]. In both cases the water is ion associated, but there is no obvious reason that such structures require this to be the case. In the case of nedocromil zinc, the long axis of the crystal is perpendicular to the hydration plane, and under crossed polarizing microscopic optics was observed to dehydrate

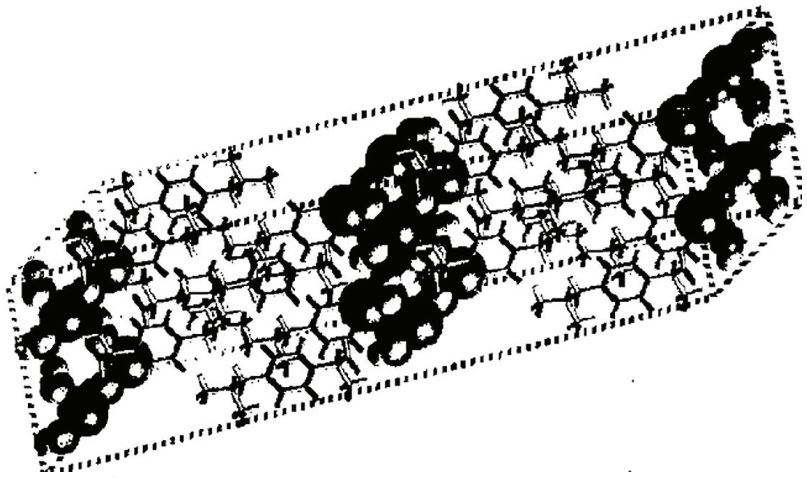

Fig. 18 Packing diagram for sodium ibuprofen with waters and sodium shown as van der Waals spheres. (From Jack Z. Gougoutas, unpublished data.)

primarily along the planar axes. This finding is consistent with the behavior cited earlier for the dehydration of channel hydrates.

3. Dehydrated Hydrates

Dehydrated hydrates may in principle belong to any of the classes just discussed, but the cases with which the author is familiar (findings not yet published) have all been either channel hydrates or "clathrate" type structures where water is the guest instead of the host in a cavity and in a nonstoichiometric amount. This subclass deals with crystals that dehydrate even at relatively high partial pressures of water. Therefore, the hydrate that forms in solution dehydrates almost immediately on removal from the mother liquor. When dehydration leaves an intact anhydrous structure that is very similar to the hydrated structure but with lower density, it is classified as a dehydrated hydrate. If there already exists an anhydrous crystalline form of the molecule, the dehydrated hydrate is classified as a polymorph.

Ulrich Griesser (University of Innsbruck) and Jack Gougoutas (Bristol-Myers Squibb) have raised the important question whether the new form is anything but another polymorph. If the water is truly a part of the crystalline structure and if in the hydrated state the waters are found, then removal of the water should change the cell parameters by some, possibly small, amount. The structure of the dehydrated form should similarly have voids large enough to accommodate some fraction of the water of hydration (hence the lower density). However, if the dehydrated form is well behaved this may not be an important distinction in the development of the compound (beyond a basic understanding of the origin of the form) unless later changes in final crystallization solvents produce solvates that do not give up their solvent quite as readily.

Another source of confusion can arise if their exists a pair of polymorphs (such as the anhydrous form and the dehydrated form) that have physicochemical properties that appear to complicate the classification of the system as enantiotropic or monotropic. For example, if density data are at odds with the relative stabilities and melting point data, then the relationship between the forms is not easily determined.

C. Class 3: Ion Associated Hydrates

Hydrates of this type contain metal ion coordinated water, and the major concern with these is the effect of the metal–water interaction on the structure of crystalline hydrates. The metal–water interaction can be quite strong relative to the other "bonding" in a molecular crystal, so that dehydration takes place only at very high temperatures [13]. Drugs with solubility, dissolution, or handling problems are most often recrystallized as Na(I), K(I), Ca(II), or Mg(II) salts and are often hygroscopic to some degree [16].

The characteristics of this hydrate class can be illustrated through a consideration of the tetra-decahydrate and tetra-dihydrate species formed by calteridol calcium (24). This compound, whose structure is shown in Fig. 19, has the chemical formula $Ca(H_2O)_2[C_{17}H_{29}N_4O_7Ca]_2$ (molecular weight 923.12) and is identified by the Cambridge reference code SQ33248. Although both the tetra-decahydrate and the tetra-dihydrate phases crystallize in the $C_{2/c}$ space group, the unit cell dimensions of these differ. For the tetra-decahydrate phase a = 33.625 Å, b = 9.517 Å, c = 20.949 Å, and β = 125.356, while for the tetra-

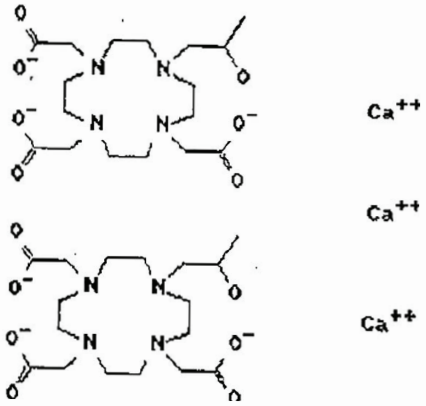

Fig. 19 Structure of calteridol calcium.

dihydrate phase a = 33.573 Å, b = 9.373 Å, c = 20.207 Å, and β = 131.620. The cell volume of the tetra-decahydrate was found to be 5467.2 $Å^3$, and the cell volume of the tetra-dihydrate phase was 4753.6 $Å^3$. Finally, the density of the tetra-decahydrate phase was determined to be 1.43 g/cm^3, while the density of the tetra-dihydrate phase was 1.44 g/cm^3. For reasons that will become clear in the following discussion, the tetra-decahydrate phase will be referred to as the reactant material, while the tetra-dihydrate phase will be referred to as the product material.

Calteridol calcium is used as a chelating excipient in a parenteral formulation and was chosen as an example for two reasons. It contains water associated with a metal cation and thus represents a Class 3 hydrate. In addition, water is also contained in channels, as with the second example. What is unique about the calteridol system is that a single crystal structure has been solved for the tetra-decahydrate (reactant) and the tetra-dihydrate (product) using the same crystal. This procedure permits an interesting look not only into the structural differences but also into the energetic differences of the water environment through thermal analysis. A similar study was performed on the dihydrate and trihydrate phases of di-sodium adenosine 5′-triphosphate [25].

Figures 20a and 20b show the packing diagrams of the initial crystal (or reactant) and the final (or product), respectively. In the packing diagrams, the water oxygens and the central calcium of the calteridol moiety are shown by their van der Waals spheres. Water molecules in the lattice (but not associated with the calcium) are represented by a sphere of one-half of their van der Waals radii, and the calteridol backbone is in stick representation. Figure 20a shows that for each calteridol, there are four water molecules associated with each central calcium, and ten lattice water molecules in each channel that run perpendicular to the plane of the figure (the b-axis). One would anticipate that the channel water would be lost more easily than would be the water associated with the cation. One reason for this is that the energy of association of water with calcium through the lone pair electrons on oxygen is greater than that of hydrogen bonding in water, and the other reason is that the loss of water in channels occurs more easily than would be expected by its interaction energy alone. Figure 20b shows the single crystal structure of the crystal after dehydration at room tem-

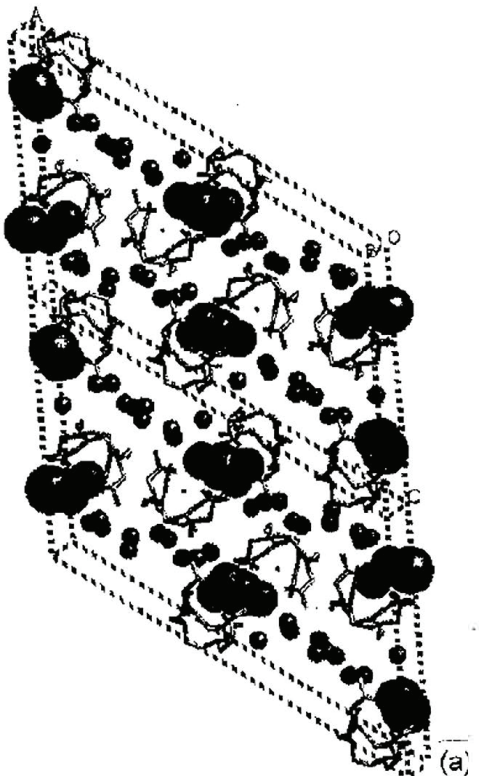

Fig. 20 Packing diagram from single crystal data for calteridol calcium (a) reactant and (b) product. The van der Waals radii are included for the water oxygens. The radii for the oxygens directly associated with the calcium are full van der Waals radii, while the lattice and channel water oxygens are shown as one-half of the van der Waals radii for illustration purposes.

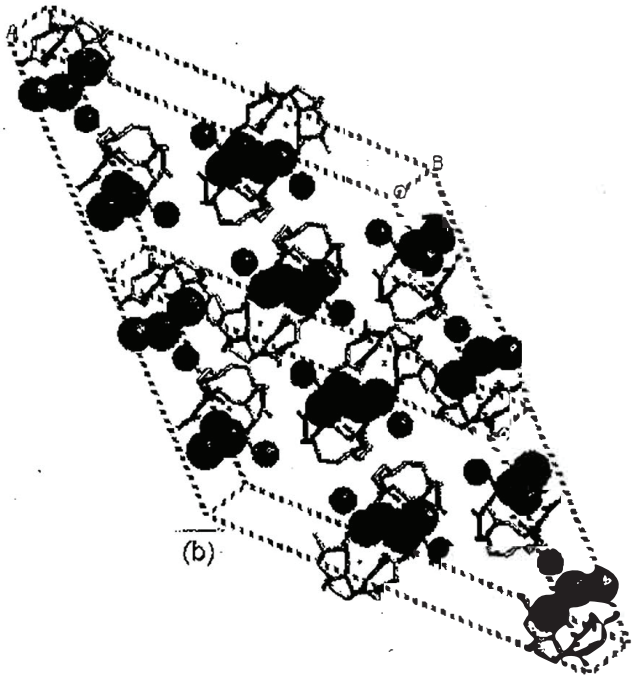

Fig. 20 Continued

perature for 6 hours. Most of the channel water (eight moles) has been lost, leaving the four calcium-associated water molecules and two water molecules in the "secondary sphere of hydration" of the calcium.

Figures 21a and b, 22a and b, and 23a and b contain the DSC, TGA, and XRPD data for the two hydrate phases of calteridol calcium. The DSC thermogram exhibits a large broad endotherm beginning at ambient temperature and peaking at approximately 75°C, which is associated with a weight loss of 13.56% (based on dry weight) or eight moles of water (calculated 13.96%). Further heating shows a smaller

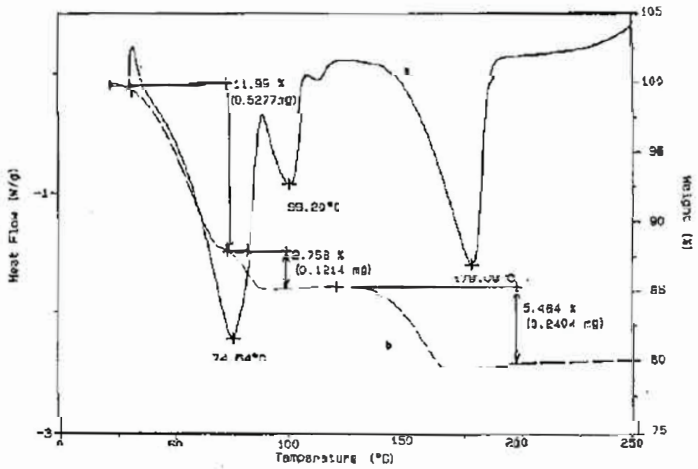

Fig. 21 (a) Differential scanning calorimetry and (b) thermogravimetric analysis thermograms for calteridol calcium tetra-decahydrate.

endotherm and weight loss corresponding to two moles of water. As the heating continues, a sharper endotherm is seen at approximately 179°C, and a weight loss corresponding to the four moles of water directly associated with the calcium ion. The molar heat of dehydration is between two and three times larger for the loss of the calcium-bound water than for the channel or lattice water.

The calculated XRPD patterns show distinctly different peak positions and intensities for the reactant and product. This is because the loss of water results in an entirely new crystal structure, unlike the situation noted for cromolyn sodium [21], in which the lattice "contracts" upon water loss without changing the crystal form. XRPD patterns collected on samples stored at 31% and 70% relative humidity show similar behavior (Figs. 22a and 23a). Notice that several diffraction peaks not present in the calculated powder pattern of the reactant are present in the measured powder pattern of material stored at 70% RH (Fig. 22). The same situation is noted for the calculated XRPD

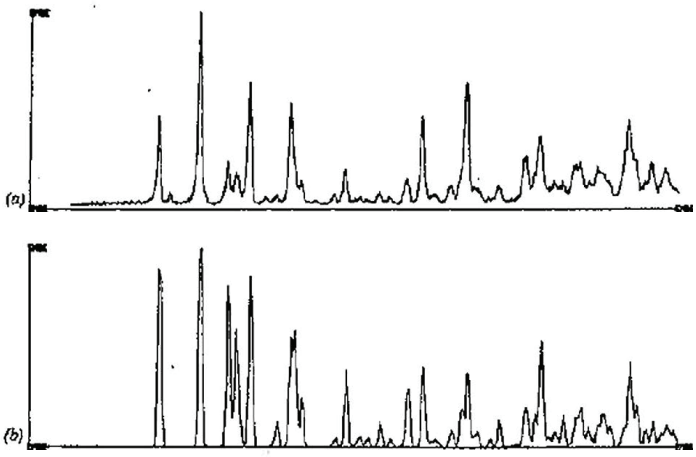

Fig. 22 (a) Measured and (b) calculated x-ray powder diffraction patterns for the calteridol calcium reactant (tetra-decahydrate).

pattern of the product pattern when compared to the measured powder pattern. This is because neither the reactant nor the product are "pure" in the sense that each contains a small amount of the other.

The thermal, Karl Fisher, and powder XRD data, coupled with the knowledge that the compound is a calcium salt, have suggested two deductions. First, the compound contains water in several crystalline environments or thermodynamic states, probably being lattice and cation associated. Second, the low-temperature water is probably contained in channels.

The characterization of pharmaceutical hydrates must be sufficient to provide confidence that the behavior of the material is predictable and reproducible. This requires the application of considerable molecular level intuition along with the available data. Data from all the techniques discussed are not always available, so in the absence of a complete data set the gaps must be filled using the types of energetic and structural principles described in the earlier chapter [1]. When the available data are consistent with what is expected from these relation-

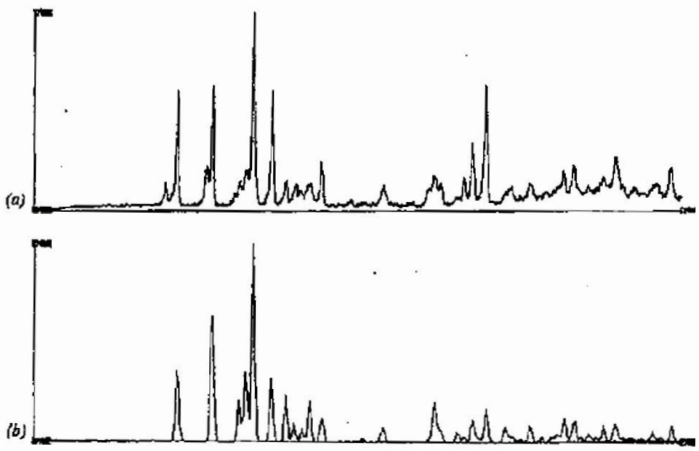

Fig. 23 (a) Measured and (b) calculated x-ray powder diffraction patterns for the calteridol calcium product (tetra-dihydrate).

ships, the behavior of crystalline hydrates should be at least qualitatively predictable.

IV. DEHYDRATION/HYDRATION KINETICS

Many models have been developed to account for the dehydration kinetics of crystalline hydrates [26]. These all assume a certain geometry and rely on some consistency of the system as the process proceeds. Often these models are indistinguishable for a given system due to experimental variation and because many structures (and, therefore, mechanisms) change during dehydration. The change in structure may also contribute to the hysteresis observed upon rehydration of a dehydrated structure. These models will not be discussed here, and the reader is referred to the literature [20] for a thorough review. The practical consequences of dehydration kinetics may be found in the activities associated with determining boundary conditions for allowable expo-

sure of bulk drug substances during development and processing; proper packaging; allowable temperature ranges for shipping, storage, and labeling of the final product; and the initial selection of a form for development.

A. Dehydration and Hydrate Class

Some general ideas of dehydration rates by class that were implicitly introduced in the classification section can be made for hydrates at room temperature and above their critical relative humidity percentage. For isolated site hydrates, rates would be very low even when heated almost to the dehydration temperature. At that temperature, the kinetics would be expected to be very rapid unless the structure collapsed and presented a barrier to loss of the last water (although this should be minimal for this class). This is because the waters are all in similar energetic environments (hydrogen bonded to drug molecules), so that when sufficient energy is supplied to free one water, there is enough to liberate them all. This is obviously a generalization, since even in an homogeneous environment there will be a relatively narrow distribution of energies.

The story should be different for channel hydrates, where the hydrogen bonding network is dominated by water–water interactions. First, one needs to revisit the concept of sigma cooperativity [27]. The idea that all the hydrogen bonds of a given water molecule may get stronger as subsequent hydrogen bonds are formed is generally accepted. The opposite situation has not been described but must apply. So if one considers a water molecule involved in 3–4 hydrogen bonds, the remaining bonds must become weaker as a bond breaks due to "inverse cooperativity." Consider the dehydration of channel hydrates. At a given temperature, the energy available for dehydration will be sufficient for some fraction of the water molecules to leave from the end on the channel. However, because the hydrogen bonding network connects through the other water molecules in the channel, and unlike the drug molecules, the inverse cooperativity now diminishes the energy with which the next water molecules are associated with the lattice. This increases the number of molecules within the range where the energy is sufficient to dislodge them from the structure. This ex-

plains both the continuous dehydration observed with onset at relatively low temperatures for channel hydrates and the relatively discrete loss for isolated site and ion associated hydrates not subject to this cascade effect.

B. Impact of Particle Size and Morphology

In general, the smaller the particle size, the more rapidly dehydration occurs. This can be justified on the basis of surface area and/or, in some cases, the existence of crystal defects. The latter is particularly true for substances that have been subjected to high-energy particle size reduction processes. The impact of morphology may be more subtle and is certainly not independent of size considerations. The balance between the two mechanisms has been a topic of discussion, but very little quantitative work has been done to elucidate the relative contribution to the dehydration process.

This topic is complicated by the reality that particle size analysis is a very subjective measurement prone to several types of sampling errors. This makes it difficult to know how to approach the problem of obtaining two morphologies of a crystalline hydrate form with the same size. This could mean the same longest dimension, the same surface area, the same aspect ratio, etc. At very small particle sizes (less than 10–20 μm), the crystallite size may not be the primary particle size, and the rate may be determined by the size of the agglomerated material. Another complication has to do with the dehydration rate measurements. As discussed earlier, the stability of the hydrated form cannot be specified without knowledge of the partial pressure (or RH) of water at each temperature of interest. Most dehydration experiments are done against very low values of relative humidity and may not be very realistic or revealing. The literature does contain some interesting studies of dehydration at various relative humidity values that clearly show the expected trends [28]. The use of moisture sorption/desorption data is also becoming more common, although most workers still use only the equilibrium values even though the kinetic data are usually available from the same experiments. The other major complication was discussed above, which is that as mechanisms change, dehydration characteristics also change.

The discussion on dehydration characteristics of the different classes suggests that, for equivalent particle size, channel hydrate dehydration kinetics should be more sensitive to changes in morphology than would be the other classes. This hypothesis should be tested by taking an isolated site and a channel hydrate, each in two morphologies with similar surface areas. The phenomena can be seen conceptually by simulating the morphology from a single crystal structure and the Bravis–Friedel–Donnay–Harker relationship [29]. Choosing the channel hydrate ampicillin trihydrate as an example, it can be seen that the water lies on the crystallographic c-axis. As the morphology changes by increasing along the channel axis (Fig. 24), the relative density of dehydration sites decreases. This should lead to slower dehydration (at least early in the process before structural changes can occur) as the average distance a water molecule must travel increases.

A precursory study was performed on two different morphologies of carbamazepine dihydrate [30]. A photomicrograph of the two habits is shown in Figs. 25a and b, which show a brick shape and a needle shape. The surface areas were not determined due to the difficulties of such determinations on easily dehydrated channel hydrates. However, the longest dimensions are close to each other, which may be perceived as an equivalent particle size (such as would be deduced by traditional sieve analysis). This would be true unless the needles pass through lengthwise. A typical problem with needles is the clogging of screens due to their stacking. The isothermal water loss (at 40°C) was followed for both samples by TGA. The results (Fig. 26) show substantial differences in the loss rates, with the needles losing mass more rapidly than do the bricks. While this example points out the possible impact of morphology on dehydration, it is apparently the opposite of what was predicted for dehydration of channel hydrates. This is possibly the result of changes in mechanism, as carbamazapine was shown to crack upon dehydration [30].

To summarize, the primary influence on dehydration rates is most likely differences in particle size (and aggregation), with morphology representing a secondary influence. However, there may be cases where morphology contributes significantly to the process and must at least be ruled out as a factor.

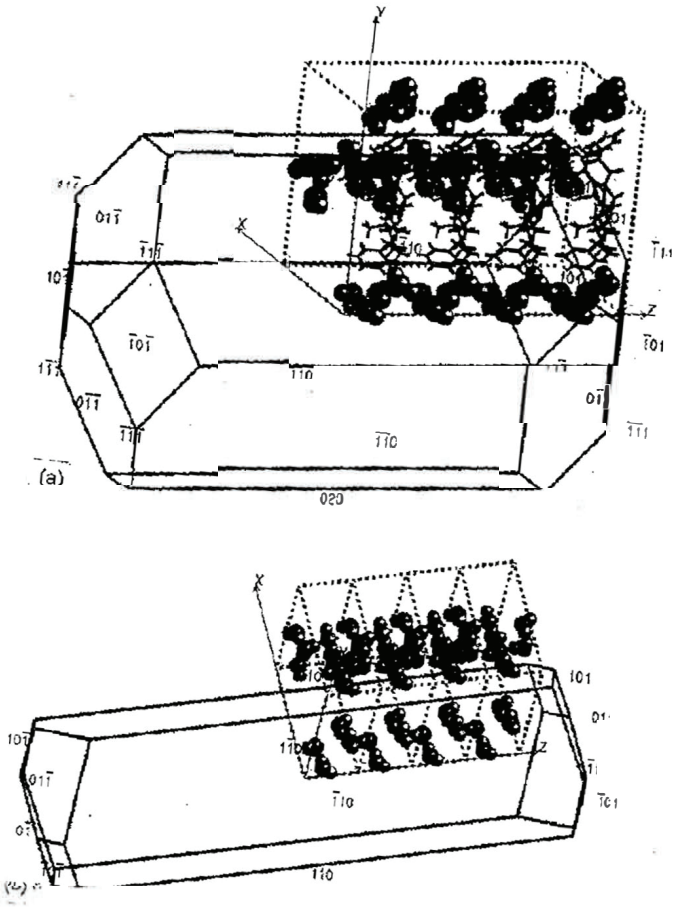

Fig. 24 (a) BFDH morphology for ampicillin, (b) computationally grown along the 110 zonal axis. (From Ref. 29.)

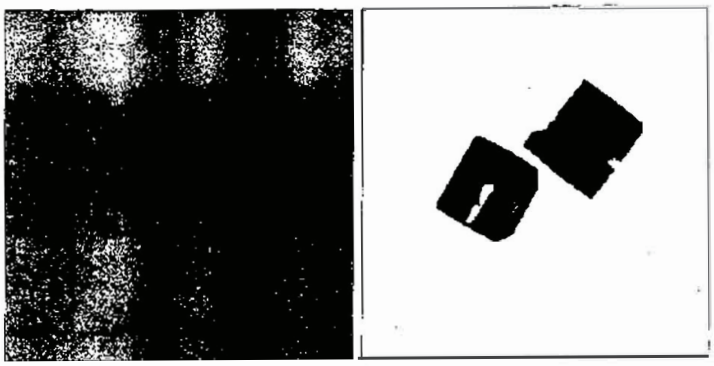

Fig. 25 Carbamazepine grown in water (left) and surfactant (right) at 52% RH for five days.

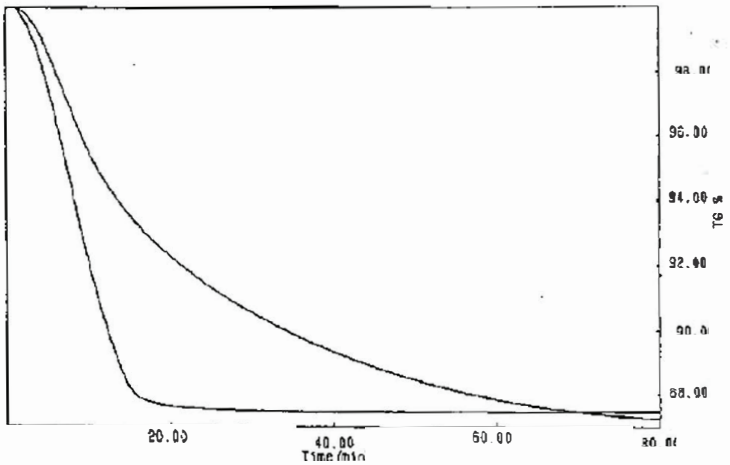

Fig. 26 Isothermal dehydration thermogravimetric analysis curves for carbamazapine dihydrate. The upper curve is for the block-like crystals grown in surfactant, and the lower is for needle-like crystals grown in water.

V. BEHAVIOR OF HYDRATES DURING PROCESSING, HANDLING, AND STORAGE

We have so far reviewed the thermodynamic concept of phase transitions and introduced a classification system for hydrates. It remains to explore where in the dosage form development process such transitions are most likely to occur and what we can say about them in light of the preceding discussion. The following discussion will be divided into situations where processing induces transitions, and transitions taking place in the final product. When appropriate, polymorphic systems are also illustrated for contrast and completeness.

A. Processing Induced Transitions

Of particular interest in pharmaceutical development is the induction of phase transitions during processing, which can occur for several possible reasons. The crystal (or amorphous) form of the bulk drug may be a metastable form that is able to "relax" to the more stable form during processing. The final state may be either a more stable polymorph or a different hydration state. The processing may kinetically trap a metastable form in the dosage form. It is also possible, in principle, that a new form may appear that is only stable in the formulation matrix. All of these possibilities are explicable in terms of G–T or G–P diagrams. This, of course, assumes that the diagrams are known, which is not typically the case. However, the combination of some data and knowledge of possible relationships should help resolve such problems.

1. Relaxation

Examples of an initially metastable phase that relaxes to a more stable phase are to be found in solutions, in suspensions, and in some solid dosage forms [31]. In solutions, the metastable form will have a higher solubility than its more stable form (and a higher free energy), so a solution of the less stable form may be supersaturated with respect to the more stable form, which then crystallizes during processing. The stable form can be a solvate or an anhydrous form. Cortisone acetate suspensions represent a well-known example where a transition to a

more stable polymorph takes place during processing. The triazinoindoles are an example where an anhydrous material transforms to a hydrate in suspension [32].

These examples are all solution-mediated transformations, which depend upon the solution phase to provide the mobility necessary to rearrange in the most stable form. Solid-state transformations are also possible when temperature and pressure changes can move the system across a phase boundary. These conditions often favor the metastable phase, however, unless there is a temperature reduction. Solid-state relaxation is more likely to be a slow (kinetically controlled) process, which is also possible during storage.

2. *Kinetic Trapping*

Processes that kinetically trap a metastable phase are not unusual. To trap a phase, one must restrict its molecular mobility once it is formed, which is easier to accomplish in a solid dosage form. Once formed, these phases may be quite stable, and some are marketed (e.g., progesterone) to take advantage of their potentially higher solubility, dissolution rate, and bioavailability. If the transformation results in a phase other than the desired one, however, concerns will arise. The two common processes in solid dosage form processing that are most likely to produce conditions conducive to kinetic trapping are tableting and wet granulation.

The heat and pressure generated during tableting has long been known to produce polymorphic and pseudopolymorphic conversions [33]. A recent example of this is found in the work of Otsuka and Matsuda, who showed that tableting can induce polymorphic transitions between the known forms of chlorpropamide [34]. Figure 27 compares the XRPD patterns for chlorpropamide tablets after repeated compression cycles with the patterns of the two polymorphs. The comparison clearly demonstrates that the compound has undergone a partial polymorphic phase transformation during the process. A similar example with a hydrate was found for SQ33600 (Fig. 16). The XRPD patterns for the surface and cross sections of regular and high-compression tablets were compared (Fig. 28), and it was obvious that the amount of change depended upon the compression force and position in the

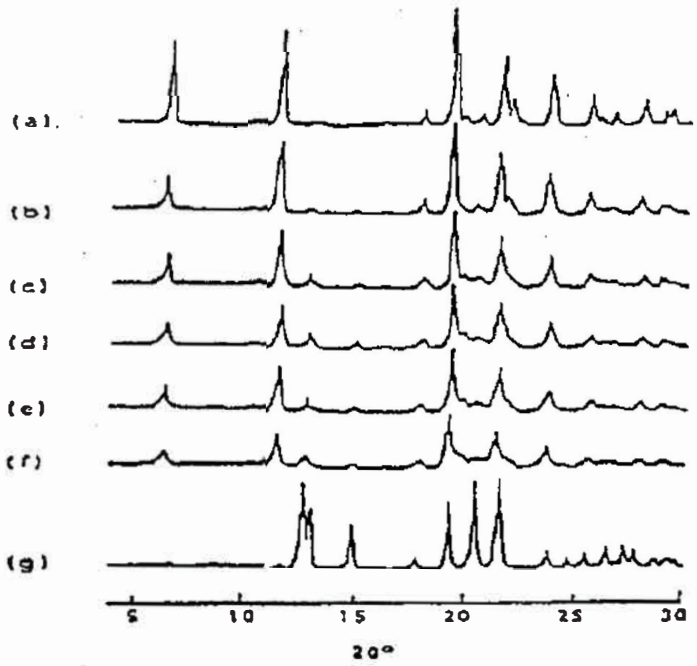

Fig. 27 Changes in chlorpropamide x-ray diffraction patterns of form A produced by repeated compression. (Reproduced with permission.)

tablet. The effect of spatial distribution may be due to the variable compression force experienced at a given depth, or it may be related to the variation in temperature with depth upon compression. It is not clear if the substance simply converted to another crystal form, or if it became amorphous due to dehydration.

Wet granulation is a particularly efficient process for kinetic trapping. In this processing methodology, one prepares a highly concentrated solution of the drug by adding hot solvent to the dry substance and mixing vigorously. The mixture is then rapidly dried, using an evaporative (cooling) process. The resulting product can exhibit char-

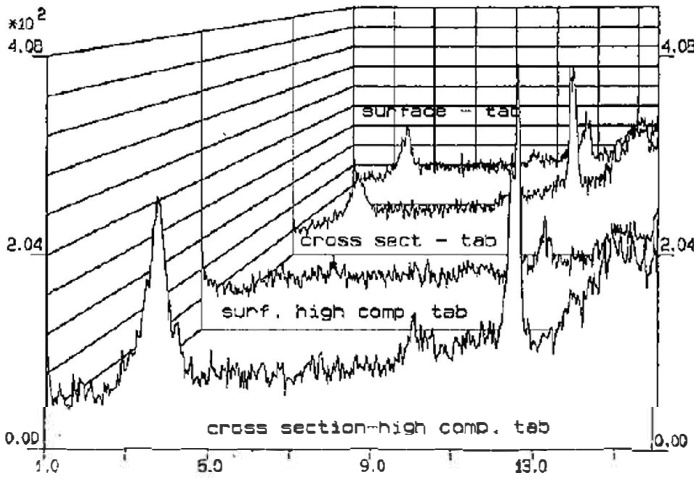

Fig. 28 X-ray powder diffraction patterns for SQ33600 tablet surface and cross section, taken from tablets formed using two different compression forces.

acteristics varying from no effect, to a mixture of forms, to a metastable crystalline form, or to a metastable amorphous form.

One example of this behavior is given by the ACE inhibitor fosinopril sodium (whose structure is provided in Fig. 29). Initially, this formulation was to be wet granulated and then compressed. Figures 30a and b show the XRPD patterns for the two known polymorphic forms of this drug. Based on the thermal data, the direction of solution mediated transformations, and thermodynamic rationale, it was determined that the forms were probably enantiotropically related, with form B being the metastable form at room temperature. During preformulation studies, it was found that the metastable B form could be produced by flash evaporation from methanol in a watch glass. This finding led to studies designed to see if one could produce form B in a laboratory granulation. Figures 31a, b, and c show the XRPD patterns for form A, form B, and the pattern generated from the lab granulation. The

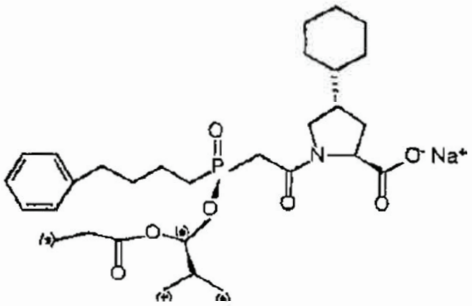

Fig. 29 Structure of fosinopril sodium.

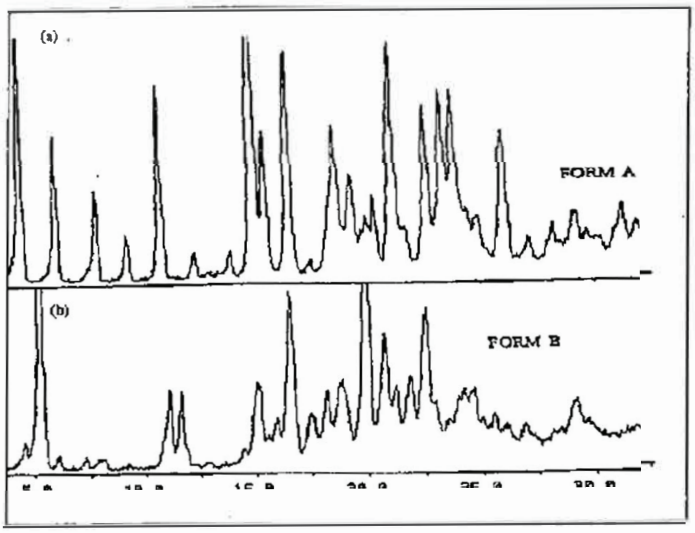

Fig. 30 X-ray powder diffraction patterns for fosinopril sodium, (a) form A and (b) form B.

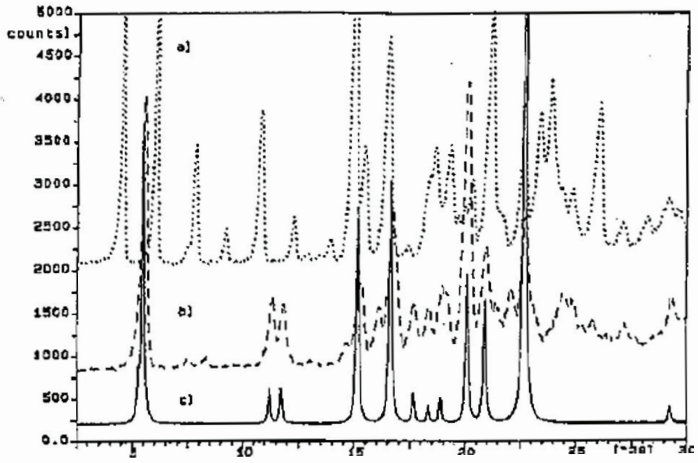

Fig. 31 X-ray powder diffraction patterns for fosinopril sodium, (a) form A, (b) form B, and (c) the material generated from a laboratory granulation.

data clearly show that the manufacturing process converted the initial form A material into the metastable form B in the dosage form. The XRPD method was found not to be sufficiently sensitive to show any form B in pilot lab tablets. Solid state ^{31}P NMR spectra (Fig. 32) clearly show the form B resonance at 55.0 ppm (form A resonating at 52.8 ppm). The process was adjusted to prevent the formation of form B.

The second example involves the channel hydrates of SQ33600. Examination of aqueous granulations of the compound with excipients showed that the crystal structure had disappeared, indicating that the drug substance had converted to the amorphous form. This is evident in the XRPD pattern comparing the dry blend to the granulate and to the tablet (Fig. 33). Apparently the tableting process also has the effect of changing the crystallinity of the compound, which further complicates the interpretation. The crystal lattice of SQ33600 is much less stable than that of fosinopril sodium, which caused significant problems in its development.

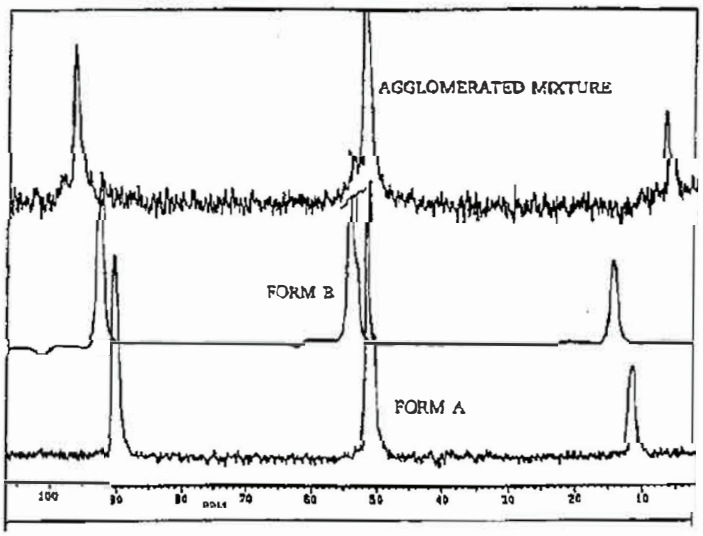

Fig. 32 Solid-state ^{31}P NMR spectra of fosinopril sodium.

B. Transitions in the Final Product

Once a final dosage form has been produced, there remains the possibility of in situ phase transitions. These can happen either because a metastable form was produced or because the ambient conditions have forced the transition. These changes can be hydration or dehydration, alterations in the polymorphic state, or amorphous-to-crystalline phase transitions.

Accelerated stability studies are potentially problematic for at least three reasons. Stress testing conditions may exceed the temperature of a polymorphic phase transition or dehydration. The use of accelerated conditions may make a relaxation of a metastable phase more rapid due to the increased molecular mobility. Finally, the relative humidity of the station may be in the range sufficient to cause a "pseudo-polymorphic" transition due to dehydration or hydration. It is sobering

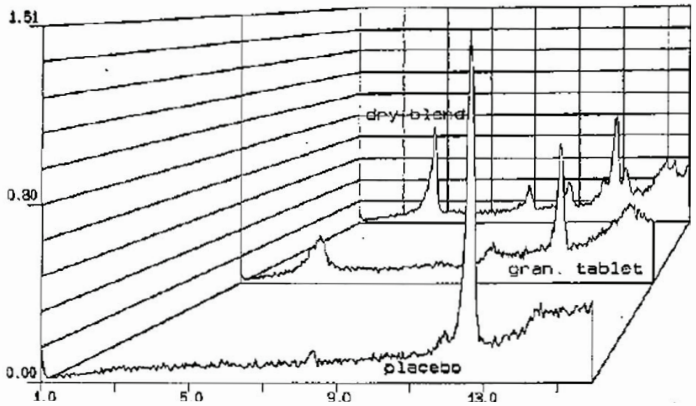

Fig. 33 X-ray powder diffraction patterns of SQ33600 dry blend (upper), granulated tablet (middle), and placebo (lower).

to think that any transition that may be observed during stability studies is also possible during storage and handling. The impact of all of these transitions is unknown until the physicochemical behavior of the related phases is determined. More and more it is becoming expected that all phase transitions that might occur in a product will be explored during the course of dosage form development.

It is easy to see from the G–T diagram of an enantiotropic polymorphic system that if the storage condition of the stable phase of a drug exceeds the transition temperature, the order of stability changes, and a new phase will form if the kinetics permit. A more common problem is exceeding the glass transition temperature of amorphous compounds (or coatings), which may in turn induce crystallization and/or other mobility related problems. The general G–T diagram (of the type shown in Fig. 3a) also shows that a metastable form at a given temperature can convert to the stable form if the kinetics are favorable. As the temperature is increased, the conversion kinetics become more favorable, even though the free energy gradient decreases. This is an unpredictable balance, but prudent workers would typically opt for

maintaining a lower temperature if their formulation included a metastable crystal form.

Using fosinopril sodium as the example, one can see evidence of such a relaxation transition. This was not observed in the final dosage form, but it probably would have occurred if the metastable form B had been chosen for development instead of the stable form A. In one study, a sample of form B was characterized by solid-state NMR, and then again after three months of storage at ambient laboratory conditions. As is evident from the data presented in Figs. 34a and b, the

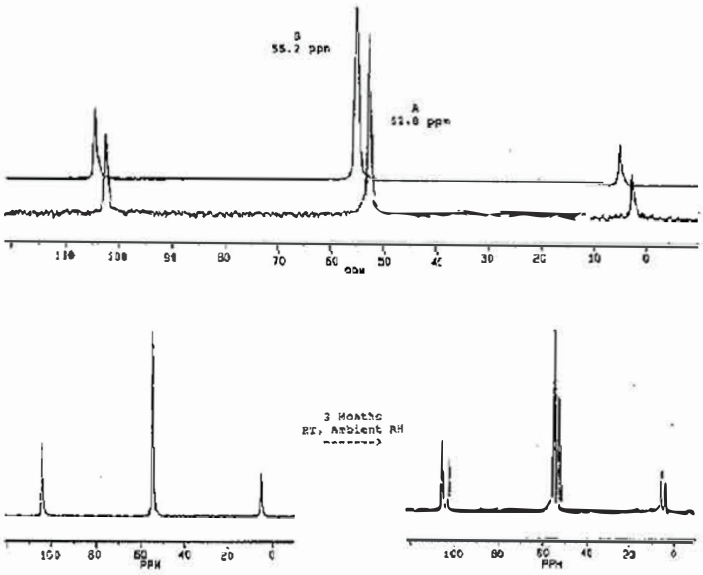

Fig. 34 Solid-state ^{31}P NMR spectra of fosinopril sodium, form A and form B (upper traces), showing the chemical shifts for the phosphorous nucleus in each form. The lower spectra show the partial interconversion from form B to form A after storage at room temperature and ambient humidity for three months.

sample had partially converted to form A in the solid state. This is a case where sufficient driving force existed for the transition (negative free energy change) but was somewhat retarded by the kinetics.

An example of a transition induced by a change in the relative humidity at a fixed temperature is again provided by SQ33600. Recall from the hydrate classification section that SQ33600 that has been equilibrated at different relative humidity values yielded XRPD patterns consistent with channel hydrate behavior. It was found that after wet granulation, the crystal form was substantially diminished and appeared to have become amorphous (see Fig. 33). When these granules were stored for five months in HDPE bottles at room temperature or at 40°C and 75% RH, the powder patterns showed that the amorphous phase had recrystallized to the forms expected under the environmental conditions (see Fig. 35). This raised concerns that the same effect could happen in tablets exposed to elevated relative humidities. An experiment was conducted in which tablets were exposed to 52% and 75% RH for four days. The resulting XRPD patterns confirmed the concern (Fig. 36). The drug had recrystallized into the hydrated forms expected from the work on the pure compound. Great care had to be taken to

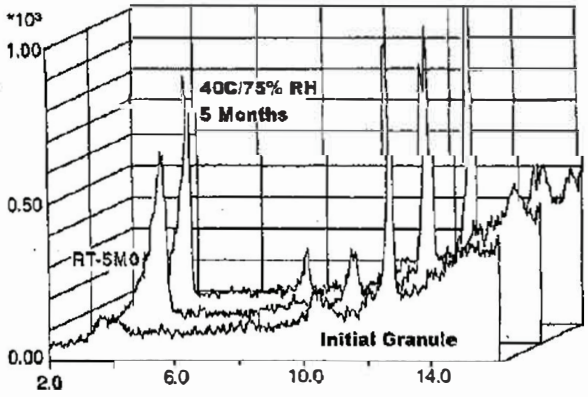

Fig. 35 X-ray powder diffraction patterns of SQ33600 granules after storage at 75% relative humidity.

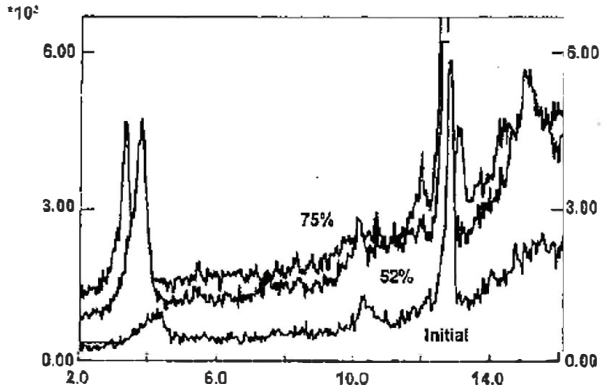

Fig. 36 X-ray powder diffraction patterns of SQ33600 tablets after their exposure for four days at 75 and 52% RH.

maintain a given hydration state and associated crystal form. This was true for clinical supplies and would obviously be true for stability studies. Fortunately, the drug solubility was sufficiently high so as to obviate any potential effects of crystal form on the dissolution rate.

C. Kinetics of Transformation

Only a few generalities can be advanced regarding the kinetics of phase transformation. Constant temperature solution mediated transformations typically proceed much faster than do those in the solid state. The rate of a solution mediated transformation is proportional to the solubility of the species involved, and this is particularly true of the relaxation transformations previously mentioned. Some transformations that proceed rapidly and are apparently occurring in the solid state may be taking place in the absorbed water layer or in the amorphous fractions. Hydrate transformations can be thought of as reactions that are not necessarily occurring in the solid state, since the water may be in the vapor phase. These may even be considered as solution mediated, which would explain the relative rapidity with which many hydration/dehydration reactions occur.

If a G–T analysis shows only a very small driving force for a solid-state polymorphic transformation, even favorable kinetics may be insufficient to allow the transition to occur rapidly. In general, the existence of favorable kinetics has more effect than does a relatively large driving force, so increasing temperature and/or pressure are the main factors over which one has any control. Obviously, relative humidity is the main factor in hydrate transformation, and here a large driving force in the partial pressure of water may enhance the kinetics by inducing mobility in the system.

VI. SUMMARY

Based on their structural characteristics, crystalline hydrates were broken into three main classes. These were (1) isolated lattice site water types, (2) channel hydrates, and (3) ion associated water types. Class 2 hydrates were further subdivided into expanded channel (nonstoichiometric) types, planar hydrates, and dehydrated hydrates. The classification of the forms together with a suitable phase diagram provides a rationale for anticipating the direction and likelihood of a transition, including transitions that may be solution mediated.

Phase transitions possible during the development process were also broadly classified. These were typified into process induced transitions (relaxation of metastable forms, and kinetic trapping of metastable forms) and transitions of the final product (accelerated stability induced changes, and relaxation of metastable forms during storage). Examples of each case were reviewed, and some specific steps in the development process were identified as being potentially problematic. Wet granulation, tableting, particle size reduction, and stress testing stability conditions were all singled out as areas of possible concern.

It is generally desirable to select the most thermodynamically stable crystal form for formulation development. This form will usually have the least liability for phase transitions and will often be the most chemically stable form. Sometimes, however, a metastable form is selected either for performance issues or because the stable form is not obtainable directly (or for historical regulatory reasons). Under these conditions, it is imperative that the solid state system be thoroughly

understood so as to avoid problems that might not have been anticipated. It is rapidly becoming expected that pharmaceutical scientists should characterize and understand their dosage form "systems" at the time when regulatory documents are filed.

Acknowledgments

The work presented here represents the efforts of many scientists. The data and insight contributions of Dr. Jack Z. Gougoutas (Bristol-Myers Squibb Institute for Medical Research) pervade this chapter. In addition, the contributions of Dr. Ann Newman, Dr. David Bugay, and Dr. Beverly Bowman (also of Bristol-Myers Squibb) make up a significant fraction of this work. Finally, I must credit the many helpful discussions I have had with Dr. David Grant (University of Minnesota), Dr. Jens Carstensen (University of Wisconsin), Dr. Steven Byrn (Purdue University), and Dr. Ulrich Griesser (University of Innsbruck).

REFERENCES

1. K. R. Morris, and N. Rodriguez-Hornado, "Hydrates," in *Encyclopedia of Pharmaceutical Technology* (J. Swarbrick, and J. Boylan, eds.), Vol. 7, Marcel Dekker, New York, 1993.
2. K. R. Morris, M. G. Fakes, A. B. Thakur, A. W. Newman, A. K. Singh, J. J. Venit, C. J. Spagnuolo, and A. T. M. Serajuddin, *Int. J. Pharm.*, *105*, 209–217 (1994).
3. H. P. Stahl, Heinrich, "The Problems of Drug Interactions with Excipients," in *Towards Better Safety of Drugs and Pharmaceutical Products* (D. D. Braimar, ed.), Elsevier/North-Holland Biomedical Press, 1980, pp. 265–280.
4. Cambridge Structural Database, V 2.3.7, 1996.
5. F. Leusen, personal communication, Molecular Simulations Inc., Cambridge, England.
6. M. Falk, and O. Knop, *Water, A Comprehensive Treatise*, Vol. 2 (F. Franks, ed.), Plenum Press, New York, 1973, pp. 55–113.
7. D. J. W. Grant, and T. Higuchi, *Solubility Behavior of Organic Compounds*, John Wiley, New York, 1990.
8. J. T. Carstensen, "Two-Component Systems," in *Solid Pharmaceutics:*

Mechanical Properties and Rate Phenomena, Academic Press, New York, 1990, pp. 102–133.
9. J. T. Carstensen, "Two-Component Systems," in *Solid Pharmaceutics: Mechanical Properties and Rate Phenomena*, Academic Press, New York, 1990, pp. 102–133.
10. H. Zhu, R. K. Khankari, B. E. Padden, E. J. Munson, W. B. Gleason, and D. J. W. Grant, *J. Pharm. Sci.*, *85*, 1026–1934 (1996).
11. J. Zhu, and D. J. W. Grant, *Int. J. Pharm.*, *139*, 33–43 (1996).
12. J. Z. Gougoutas, personal communication.
13. I. Dzidic, and P. Kebarle, *J. Phys. Chem.*, *74*, 1466–1474 (1970).
14. W. Mikenda, *J. Mol. Struct.*, *147*, 1–15 (1986).
15. H. D. Lutz, "Bonding and Structure of Water Molecules in Solid Hydrates," in *Structure and Bonding 69* (Leeberg, ed), Springer-Verlag, Berlin, Heidelberg, 1988, pp. 97–125.
16. S. M. Berge, L. D. Bighley, and D. C. Monkhouse, *J. Pharm. Sci.*, *66*, 1–18 (1977).
17. K. Florey, "Cephradine," in *Analytical Profiles of Drug Substances*, Vol. 2 (K. Florey, ed.), Academic Press, New York, 1973, pp. 1–62.
18. H. G. Brittain, D. E. Bugay, S. J. Bogdanowich, and J. DeVincentis, *Drug Dev. Ind. Pharm.*, *14*, 2029–2046 (1988).
19. E. Ivashkiv, "Ampicillin," in *Analytical Profiles of Drug Substances*, Vol. 2 (K. Florey, ed.), Academic Press, New York, 1973, pp. 1–62.
20. S. R. Byrn, *Solid-State Chemistry of Drugs*, Academic Press, New York, 1982.
21. J. S. G. Cox, G. D. Woodard, and W. C. McCrone, *J. Pharm. Sci.*, *6*, 1458–1465 (1971).
22. K. R. Morris, A. W. Newman, D. E. Bugay, S. A. Ranadive, A. K. Singh, M. Szyper, S. A. Varia, H. G. Brittain, and A. T. M. Serajuddin, *Int. J. Pharm.*, *108*, 195–206 (1994).
23. J. Zhu, B. E. Padden, E. J. Munson, and D. J. W. Grant, *J. Pharm. Sci.*, *86*, 418–428 (1997).
24. J. Z. Gougoutas, unpublished data.
25. Y. Sugawara, N. Kamiya, H. Iwasaki, T. Ito, and Y. Satow, *J. Am. Chem. Soc.*, *113*, 5440–5445 (1991).
26. D. Giron, *Acta Pharm. Jugosl.*, *40*, 95–147 (1990).
27. L. Pauling, *The Nature of the Chemical Bond*, 3d ed., Cornell Univ. Press, New York, 1960, Chapter 12.
28. A. K. Galwey, G. M. Laverty, N. A. Baranov, and B. Okhotnikov, *Phil. Trans. Royal. Soc. London*, *A347*, 157–184 (1994).

29. Cerius² Version 3.5 (Morphology predictor), Molecular Simulations Inc., San Diego, CA (1997).
30. D. Murphy, Ph.D. dissertation, Univ. of Michigan, 1997.
31. J. Haleblian, and W. C. McCrone, *J. Pharm. Sci.*, *58*, 911–929 (1969).
32. J. Haleblian, *J. Pharm. Sci.*, *64*, 1269–1288 (1975).
33. M. G. Wall, *Pharm. Manuf.* (February), 33–42 (1986).
34. M. Otsuka, and Y. Matsuda, *Drug Dev. Ind. Pharm.*, *19*, 2241–2269 (1993).